Pair tunneling, phase separation, and dimensional crossover in imbalanced fermionic superfluids in a coupled array of tubes

Kuei Sun and C. J. Bolech

Pair tunneling, phase separation and dimensional crossover in imbalanced fermionic superfluids in a coupled array of tubes

Kuei Sun and C. J. Bolech

Department of Physics, University of Cincinnati, Cincinnati, Ohio 45221-0011, USA

We study imbalanced fermionic superfluids in an array of one dimensional tubes at the incipient dimensional crossover regime, wherein particles can tunnel between neighboring tubes. In addition to single-particle tunneling (ST), we consider pair tunneling (PT) that incorporates the interaction effect during the tunneling process. We find that with an increase of PT strength, a system of low global polarization evolves from a structure with a central Fulde-Ferrell-Larkin-Ovchinnikov (FFLO) state to one with a central BCS-like fully-paired state. For the case of high global polarization, the central region exhibits pairing zeros embedded in a fully-paired order. In both cases, PT enhances the pairing gap, suppresses the FFLO order and leads to spatial separation of fully-paired and fully-polarized regions, same as in higher dimensions. Thus, we show that PT beyond second-order ST processes is of relevance to the development of signatures characteristic of the incipience of the dimensional crossover.

I. INTRODUCTION

Superconductivity and ferromagnetism are two ubiquitous but competing phenomena in condensed matter systems. Spin imbalance and magnetic field induced by ferromagnetism tend to suppress Cooper pairing, which is responsible for superconductivity. For more than four decades an interesting phase, the Fulde-Ferrell-Larkin-Ovchinnikov (FFLO) state [1, 2], has been suggested as the concurrence of both ferromagnetic and oscillatory superconducting orders [3, 4], but its direct confirmation is still elusive. Recently, owing to the capability of controlling particle densities, tuning interactions and cooling into quantum degeneracy [5, 6], cold atomic systems have become a promising platform for searching for FFLO order [7, 8]. In experiments of trapped Fermi gases, density profiles that reflect the interplay of spin imbalance (ferromagnetic order) and Cooper pairing have been observed [9–11]. In addition, experiments have also revealed significant dimensional dependence of the profiles: in three dimensions (3D) a fully paired profile takes place at the trap center and a polarized profile does off center [9, 10], while in one dimension (1D) the central region is always polarized [11]. These observations agree with theoretical studies of the FFLO state in 1D and the trap-induced phase separation in 3D [12–19], but the marked difference between these two limits also raises the need for understanding the intermediate regime. Several works have focused on the dimensional crossover regime of various kinds of continuous systems [20–25] or Hubbard lattices [26, 27], but with a different emphasis than the present work.

In this paper, we study a realizable system of a two dimensional optical lattice array of 1D tubes, subject to a global trapping potential [11, 28, 29]. The incipient dimensional crossover regime of this system, which can be experimentally accessed by gradually lowering the lattice depth, is modeled by incorporating the kinetics of single-particle tunneling (ST) as well as a key ingredient
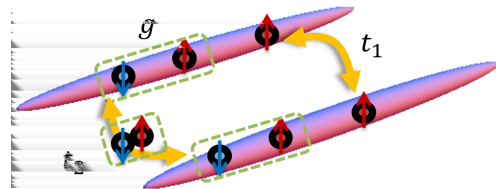

FIG. 1: (color online) Illustration of single particle and pair tunneling processes, t_1 and t_2, respectively, between two neighboring tubes in the array. On each tube, two opposite-spin atoms can form a bound pair (circled in the graph) in the presence of an attractive interaction g. The circled pair in the middle indicates that the two atoms remain paired during the t_2 process.

representing the tunneling of paired opposite-spin atoms – pair tunneling (PT) – between neighboring tubes (as illustrated in Fig. 1). The ST leads to an interesting magnetic compressible-incompressible phase transition analogous to that in the Bose-Hubbard model (discussed in Ref. [25]) but is not responsible for certain observed signatures in the profiles at the dimensional crossover regime (that will be shown below). By considering PT, we are able to describe the incipient evolution of profiles from 1D toward 3D and obtain the emerging signatures of the dimensional crossover at various global polarizations, such as the inversion of the fully-paired and polarized centers as well as the growing spatial separation between the fully-paired and fully-polarized regions.

The paper is outlined as follows. In Sec. II, we discuss the microscopic physical cause of the PT and evaluate its strength using a two-channel model. In Sec. III, we construct a model Hamiltonian and apply a Bogoliubov-de Genne (BdG) treatment to solve for the density and pairing profiles of the system. In Sec. IV, we present the results and discuss their physical meanings associated with PT. Finally we summarize our work in Sec. V.
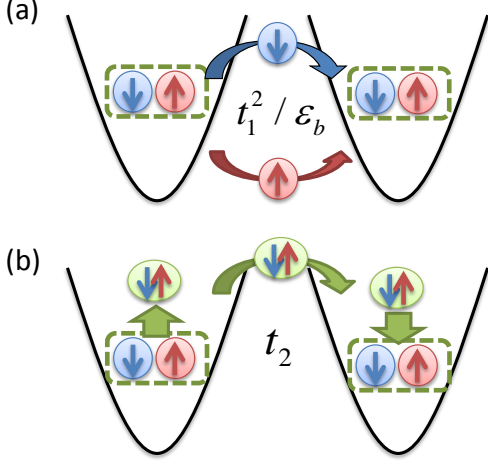
FIG. 2: (color online) Illustration of two microscopic kinetics of the pair tunneling in optical lattices. (a) Two atoms of a pair split, separately tunnel to the other site and re-bind, as a second-order process of strength t_1^2/ϵ_b in the single-particle tunneling model. (b) Atoms bind via a pervasive Feshbach resonant effect during the whole tunneling event, with the effective pair tunneling strength t_2.

II.   PHYSICS OF PAIR TUNNELING

For free fermions in a lattice potential, the inter-site kinetics is well described by ST processes of strength t_1 [30]. For an attractively interacting case where two opposite-spin atoms form a pair of binding energy ϵ_b, the kinetics of the pair tunneling would, in principle, be incorporated as a process in which the two atoms of a pair split, separately tunnel to the other site and re-bind (see illustration in Fig. 2a). This is contained in the ST model as a second order process of strength t_1^2/ϵ_b and accounts for the Josephson phenomena in the presence of superfluid orders, cf. [22].

However, in cold-atom experiments, the interaction is induced via a Feshbach resonance [31], which is controlled by the tuning of a magnetic field affecting the hyperfine energy splittings. Because the field is applied throughout the system, the interaction that leads to pairing exists on and *between* lattice sites. Therefore, we expect that atoms that remain paired during the whole tunneling event can be another viable process (see illustration in Fig. 2b). Such process can be described as tunneling of the paired atoms, with strength denoted as t_2.

One can estimate t_2 around the Feshbach resonant regime using a two-channel model [6, 7, 31] that incorporates atomic and molecular degrees of freedom, ψ_σ and ϕ, respectively. In optical lattices [32–34], the partition function of the system is

$$\mathcal{Z} = \int D\{\psi_{\sigma i}, \bar{\psi}_{\sigma i}\} D\{\phi_i, \bar{\phi}_i\} e^{-\int d\tau (S_a + S_m)}, \qquad (1)$$

where S_a contains terms associated only with the atomic degrees of freedom, including the atomic tunneling as well

as any bare inter-atomic interaction, and

$$S_m = -t_m \sum_{\langle ij \rangle, \sigma} \bar{\phi}_i \phi_j - \mu_m \sum_{i, \sigma} \bar{\phi}_i \phi_i$$
$$+ U_{am} \sum_i \left(\bar{\phi}_i \psi_{\downarrow i} \psi_{\uparrow i} + \text{H.c.} \right) \qquad (2)$$

involves the molecular tunneling t_m, molecular chemical potential μ_m, and the atom-molecule coupling U_{am}. Here we assume the inter-molecular interaction is weak such that a mean-field approximation, $\bar{\phi}_i \bar{\phi}_i \phi_i \phi_i \rightarrow \langle \bar{\phi}_i \phi_i \rangle \bar{\phi}_i \phi_i$, can be applied to incorporate the interaction as effective contributions to the chemical potentials. We integrate out the molecular variable ϕ in Eq. (1) and obtain

$$\mathcal{Z} = \int D\{\psi_{\sigma i}, \bar{\psi}_{\sigma i}\} e^{-\int d\tau (S_a + S_a')}, \qquad (3)$$

where S_a' is expanded as

$$S_a' = \frac{U_{am}^2}{\mu_m} \left[-\sum_i \bar{\psi}_{\uparrow i} \bar{\psi}_{\downarrow i} \psi_{\downarrow i} \psi_{\uparrow i} \right.$$
$$\left. - \frac{t_m}{\mu_m} \sum_{\langle ij \rangle, \sigma} \bar{\psi}_{\uparrow i} \bar{\psi}_{\downarrow i} \psi_{\downarrow j} \psi_{\uparrow j} + \mathcal{O}\left(\frac{t_m^2}{\mu_m^2}\right) \right]. \quad (4)$$

The first term in Eq. (4) can be treated as a resonant contribution to the inter-atomic interaction [48], while the second one appears as PT. Therefore, we obtain

$$t_2 = \frac{U_{am}^2}{\mu_m^2} t_m. \qquad (5)$$

Considering the tunneling strength in optical lattices given by $\frac{4}{\sqrt{\pi}} E_R (V_0/E_R)^{3/4} \exp[-2\sqrt{V_0/E_R}]$ with V_0 being the optical-lattice depth and E_R being the recoil energy [35, 36], we find

$$\frac{t_2}{t_1} = \sqrt{2} \frac{U_{am}^2}{\mu_m^2} \exp\left[-2\sqrt{\frac{V_0}{E_R}}\right] \qquad (6)$$

This expression shows that t_2 has the same sign as t_1 and can vary at fixed t_1 (or fixed lattice geometry) through the tuning of U_{am} and μ_m. We also see that even if the molecular tunneling is smaller than the atomic tunneling ($t_m < t_1$), t_2 can be comparable with or even larger than t_1 in relatively shallow lattices and near the Feshbach resonance (large U_{am} and small μ_m [37]). Realistic values can be estimated as $U_{am} = \sqrt{4\pi\hbar^2 \delta\mu W |a_b|/m} \int w_m(\mathbf{r} - \mathbf{r}_i) w_a^2(\mathbf{r} - \mathbf{r}_i) d\mathbf{r}$ and $\mu_m = \delta\mu\delta B$ (taking the bare molecular limit) [31–33], where $\delta\mu$ is the differential magnetic moment, W is the resonance width, a_b is the background scattering length, w_m (w_a) are the molecular (atomic) Wannier wave functions on site i, and δB is the detuning of the magnetic field. In an ongoing experiment using a setup as in Ref. [11] with $V_0 \sim 7E_R$ [29], we can expect $t_2/t_1 \sim 1$

given $|U_{am}/\mu_m| \sim 10$ (or $\delta B < 1.6G$). We remark that perturbative-RG analysis starting from 1D becomes unreliable in this parameter regime.

In addition, our system shows pervasive pairing effects and is thus different from an array of Josephson junctions that lack the pairing mechanism in the insulating barriers between the superconductors. Therefore, by providing extra channels for Josephson-type tunneling, the PT processes can lead to an enhancement of the superfluid order and its cross-tube coherence, anticipating the dimensional crossover regime. Notice that we focus here on the leading processes in the lowest Bloch band, which has been shown capable of describing well the realized optical lattice systems [35]. We point out that incorporating higher-order, higher-band or inter-band processes are possible immediate extensions of our model [33, 38], necessary to explore even wider optical-lattice regimes.

III. BDG CALCULATION

Incorporating both the ST and PT effects, the tube lattices occupied by up-spin (majority) and down-spin (minority) atoms, $\hat{\psi}_{\sigma=\uparrow/\downarrow,\mathbf{r}}(z)$, are hence described by the microscopic Hamiltonian

$$
\begin{aligned}
H &= \int_z \sum_{\mathbf{r}} \Big(\sum_\sigma \hat{\psi}_{\sigma\mathbf{r}}^\dagger H_\sigma^0 \hat{\psi}_{\sigma\mathbf{r}} - g \hat{\psi}_{\uparrow\mathbf{r}}^\dagger \hat{\psi}_{\downarrow\mathbf{r}}^\dagger \hat{\psi}_{\downarrow\mathbf{r}} \hat{\psi}_{\uparrow\mathbf{r}} \Big) \\
&+ \int_z \sum_{\langle \mathbf{rr'} \rangle} \Big(-t_1 \sum_\sigma \hat{\psi}_{\sigma\mathbf{r'}}^\dagger \hat{\psi}_{\sigma\mathbf{r}} - t_2 \hat{\psi}_{\uparrow\mathbf{r'}}^\dagger \hat{\psi}_{\downarrow\mathbf{r'}}^\dagger \hat{\psi}_{\downarrow\mathbf{r}} \hat{\psi}_{\uparrow\mathbf{r}} \Big), (7)
\end{aligned}
$$

with the $\hat{z}$ direction along the tube's axis and $\mathbf{r} = (x, y)$ denoting tube indexes in the plane perpendicular to $\hat{z}$. The one-particle Hamiltonian, $H_\sigma^0 = -(\hbar^2/2m)\partial_z^2 + m(\omega_r^2 r^2 + \omega z^2)/2 - \mu_\sigma$, includes the kinetic energy in the $\hat{z}$ direction, the global trapping potential and the spin-dependent chemical potentials. The on-tube coupling constant (taken positive for attractive interaction) is given as $g = -2\hbar^2 a_s/[m\ell^2(1 - 1.033a_s/\ell)]$ in the highly elongated tube limit, with a_s being the two-body s-wave scattering length and ℓ being the oscillator length of the transverse confinement in a tube [39]. In the tube array of lattice spacing d, $\ell \sim (V_0/E_R)^{-1/4} d/\pi$. The ST (PT) of strength t_1 (t_2), takes place between nearest-neighbor tubes, $\langle \mathbf{rr'} \rangle$.

Applying the BdG mean-field theory [40], (which has successfully described tube lattices without PT [25] and a variety of tube confinements [12, 15, 19, 21, 41, 42]), we construct a mean-field Hamiltonian, H_M, by correspondingly replacing the quartic operators in Eq. (7) with quadratic ones coupled to three different mean fields,

$$
\begin{aligned}
H_M &= \int_z \sum_{\mathbf{r}} \Big[\sum_\sigma \hat{\psi}_{\sigma\mathbf{r}}^\dagger (H_\sigma^0 + U_{\sigma\mathbf{r}}) \hat{\psi}_{\sigma\mathbf{r}} \\
&+ (\Delta_\mathbf{r} \hat{\psi}_{\uparrow\mathbf{r}}^\dagger \hat{\psi}_{\downarrow\mathbf{r}}^\dagger + \text{H.c.}) \Big] + \int_z \sum_{\langle \mathbf{rr'} \rangle, \sigma} \mathcal{T}_{\sigma\mathbf{rr'}} \hat{\psi}_{\sigma\mathbf{r'}}^\dagger \hat{\psi}_{\sigma\mathbf{r}}.
\end{aligned}
$$

$$(8)$$

Here the Hartree field, $U_{\sigma\mathbf{r}}(z)$, and the BCS gap field, $\Delta_\mathbf{r}(z)$, are standard variational fields in previous BdG studies. We introduce a tunneling field, $\mathcal{T}_{\sigma\mathbf{rr'}}(z)$, as a new ingredient to describe the effective tunneling under the influence of both t_1 and t_2. We rotate H_M into the quasiparticle basis, $\hat{\gamma}_n$, through a Bogoliubov transformation, $\hat{\psi}_{\sigma\mathbf{r}}(z) = \sum_n [u_{n\sigma\mathbf{r}}(z)\hat{\gamma}_{n\sigma} - \sigma v_{n\sigma\mathbf{r}}^*(z)\hat{\gamma}_{n,\bar{\sigma}}^\dagger]$ (where $\bar{\sigma} = -\sigma$), and derive extended BdG equations for the quasiparticle wave functions, $u_{n\sigma}$ and $v_{n\sigma}$, as well as the corresponding energies, $\epsilon_{n\sigma}$. The condition, $\delta \langle H - TS \rangle = 0$, which guarantees solutions of an equilibrium state at temperature T, leads to the self-consistent relations,

$$
U_{\sigma\mathbf{r}} = -g \left\langle \hat{\psi}_{\bar{\sigma}\mathbf{r}}^\dagger \hat{\psi}_{\bar{\sigma}\mathbf{r}} \right\rangle = -g \sum_n |u_{n\bar{\sigma}\mathbf{r}}|^2 f_{n\sigma}, \quad (9)
$$

$$
\begin{aligned}
\Delta_\mathbf{r} &= -g \left\langle \hat{\psi}_{\downarrow\mathbf{r}} \hat{\psi}_{\uparrow\mathbf{r}} \right\rangle - t_2 \sum_{\mathbf{r'}}{}' \left\langle \hat{\psi}_{\downarrow\mathbf{r'}} \hat{\psi}_{\uparrow\mathbf{r'}} \right\rangle \\
&= \sum_n \left(-g u_{n\uparrow\mathbf{r}} v_{n\downarrow\mathbf{r}}^* - t_2 \sum_{\mathbf{r'}}{}' u_{n\uparrow\mathbf{r'}} v_{\downarrow n\mathbf{r'}}^* \right) f_{n\uparrow},
\end{aligned}
$$

$$(10)$$

$$
\begin{aligned}
\mathcal{T}_{\mathbf{rr'}\sigma} &= -t_1 - t_2 \left\langle \hat{\psi}_{\bar{\sigma}\mathbf{r'}}^\dagger \hat{\psi}_{\bar{\sigma}\mathbf{r}} \right\rangle \\
&= -t_1 - t_2 \sum_n u_{n\bar{\sigma}\mathbf{r'}}^* u_{n\bar{\sigma}\mathbf{r}} f_{n\bar{\sigma}},
\end{aligned}
$$

$$(11)$$

where $f_{n\sigma} = [\exp(\epsilon_{n\sigma}/k_B T) + 1]^{-1}$ is the Fermi distribution function and $\sum_{\mathbf{r'}}'$ runs over all tubes at $\mathbf{r'}$ next to $\mathbf{r}$. Equation (10) shows that the magnitude of the pairing gap is enhanced by t_2 in uniform lattices where $\langle \hat{\psi}_{\downarrow\mathbf{r}} \hat{\psi}_{\uparrow\mathbf{r}} \rangle = \langle \hat{\psi}_{\downarrow\mathbf{r'}} \hat{\psi}_{\uparrow\mathbf{r'}} \rangle$ (and would also be in trapped systems, as expected through a local density approximation argument). This enhancement tends to stabilize the fully paired phase against being invaded by unpaired majority atoms; in analogy to the Meissner effect [43] which prevents the superconducting bulk from being penetrated by the magnetic field. When $t_2 = 0$, $\mathcal{T} = -t_1$ turns Eq. (8) back to that for the Hamiltonian with only ST (discussed in Ref. [25]). We numerically solve the BdG equation and apply the solutions to calculate the spatial profiles of pairing gap Δ, total density $\rho = \rho_\uparrow + \rho_\downarrow$, and spin imbalance (or magnetization) $s = \rho_\uparrow - \rho_\downarrow$; where $\rho_\sigma = \langle \hat{\psi}_\sigma^\dagger \hat{\psi}_\sigma \rangle$ is the density profile of σ species. In Sec. IV we present the results for a spherically trapped system ($\omega_r = \omega$).

IV. RESULTS

From now on, we take a realistic setup $d = -a_s = 0.5\mu$m for ^{6}Li systems in the Feshbach resonant regime and use the binding energy $\epsilon_b = mg^2/4\hbar^2$ as the energy unit for the following results. We look at the influence of t_2 at fixed $t_1 = 0.014\epsilon_b$, the latter corresponding to a typical lattice depth of $7E_R$ and thus into the dimensional crossover regime. In Fig. 3, we plot the axial profiles of ρ, s and the average of $|\Delta|$ by tracing out the $\mathbf{r}$ degree of
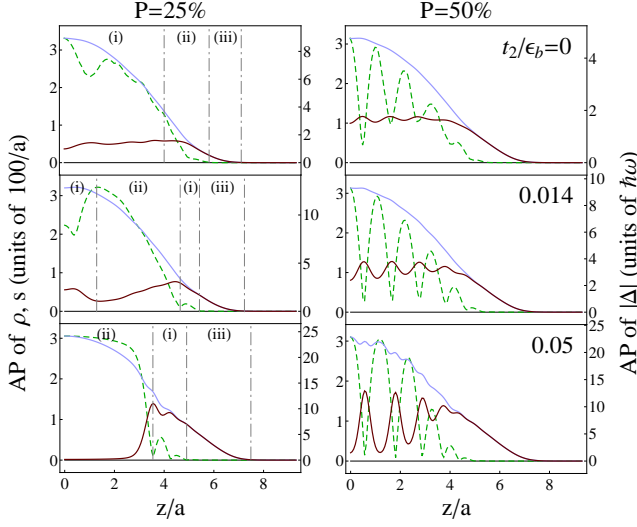
FIG. 3: (color online). Axial profiles (AP) of total density ρ, spin imbalance s, (solid light blue and dark red curves, respectively, axis on the left of graph), and average magnitude of pairing gap $|\Delta|$ (dashed green curve, axis on the right of graph) for various pair-tunneling strengths t_2, and global polarizations P. Rows from top to bottom correspond to $t_2 = 0$, $0.014\epsilon_b$, and $0.05\epsilon_b$, respectively; while the left and right columns correspond to $P = 0.25$ and 0.5, respectively. On the left column the dash-dotted lines demarcate regions of (i) FFLO, (ii) BCS-like fully-paired, and (iii) fully-polarized states. The data obtained were for systems of 2400 particles in a 10×10 tube array with global trapping frequency $\omega = 0.0625\epsilon_b/\hbar$ (which defines the oscillator length in the $\hat{z}$ direction, $a = \sqrt{\hbar/m\omega}$), single particle tunneling $t_1 = 0.014\epsilon_b$, and temperature $T = 0.1\epsilon_b$. These parameters are similar to those used in experiments.

FIG. 4: (color online). Value of the gap function (in units of $\hbar\omega$) at the center of each tube ($z = 0$) for various t_2 and P (convention as presented in Fig. 3). Here we show data for 5×5 tubes in the fourth quadrant of the 10×10 tube array, in which the top left entry of each panel corresponds to the most central tube. The other quadrants are similar due to 4-fold rotational symmetry.

freedom. The first and second columns correspond to a lower global polarization of $P = 25\%$ (LP) and a higher one of $P = 50\%$ (HP), respectively [49]. From top to bottom rows, t_2 is chosen to be either zero, comparable to t_1, or large compared with t_1, respectively. We see that in the LP case at $t_2 = 0$, the axial profile exhibits (i) an FFLO center with oscillatory Δ, (ii) a BCS-like shoulder with non-oscillatory Δ, and (iii) a normal tail having zero Δ. At the intermediate t_2 value, this tri-layered structure remains. However, the FFLO center shrinks, the BCS-like region extends toward the center accompanied with a drop in imbalance, and the normal tail grows. This indicates a transfer of unpaired majority atoms from the center to the tail, implying an enhancement of a Meissner-like effect in the central region. We notice that the gap profile develops small ripples between the BCS-like shoulder [(ii)] and the normal tail [(iii)], suggesting the incipience of an FFLO layer [(i)] here. At the large t_2 value, the FFLO center is completely conquered by the BCS-like state and disappears, leaving a large fully-polarized tail and a thin FFLO layer in between them. Because the FFLO and BCS centers are distinctive of 1D [11] and 3D [9, 10] trapped systems,
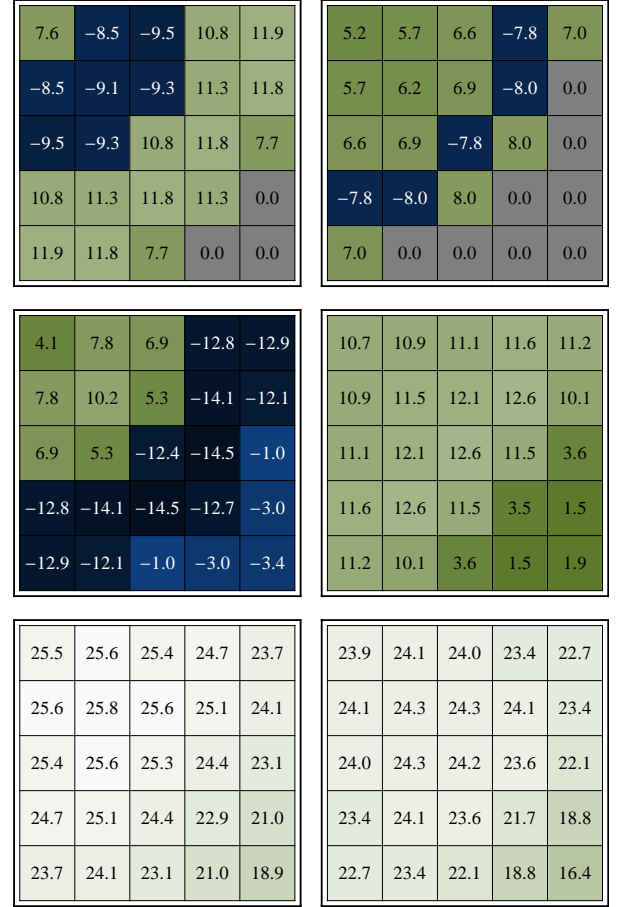
respectively, this result shows the evolution of the system from 1D toward 3D, driven by t_2 (compared with increasing t_1).

In the HP case, the system always has a center with oscillatory Δ and a fully-polarized normal tail. In the oscillatory-pairing region, the imbalance profile exhibits characteristic out-of-phase oscillations, with the concurrence of local minima (maxima) of s and local maxima (minima) of $|\Delta|$. This behavior is due to the competition between superfluid and ferromagnetic orders. An increase in t_2 enhances this competition, augmenting the magnitude of the out-of-phase oscillations and repelling a portion of the unpaired majority to the normal tail region. At large t_2 ($= 0.05\epsilon_b$), the oscillations are large enough that the minima of s are almost zero. Such case is less like an FFLO state (oscillatory pairing accompanied with finite polarization), but more like spatial alternation of fully-paired superfluid and highly polarized normal gas. This phenomena, analogous to the phase
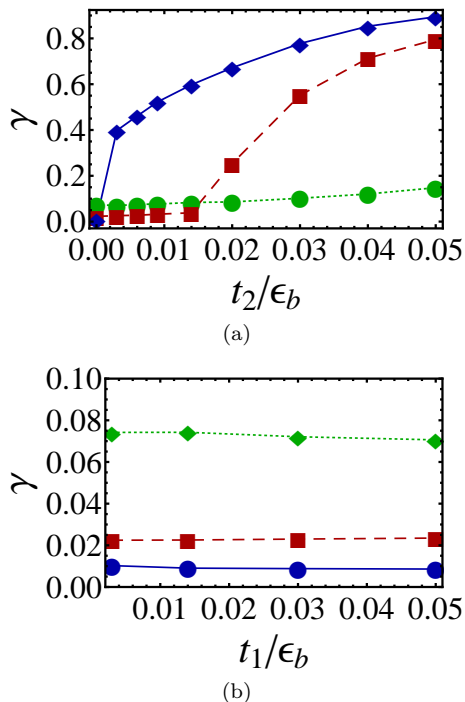
FIG. 5: (color online) The combined fraction of particles in the highly paired ($s/\rho < 5\%$) and highly polarized ($s/\rho > 95\%$) regions, γ, vs t_2 (a) or t_1 (b) with the other fixed. The solid blue, dashed red, and dotted green curves represent cases with global polarization $P = 12.5\%$, 25% and 50%, respectively.

separation in the LP case, is taken as a signature of the dimensional crossover between 1D and 3D at higher polarizations. We also notice that the structure of the profiles is reminiscent of that of a system with vortex cores embedded in a superfluid bulk.

We find that PT affects the pairing order not only along but also across the tubes. Figure 4 shows the value of the gap function at the center of each tube ($z = 0$) in a 10×10 tube array. The left (right) column corresponds to the LP (HP) case, while, from top to bottom, rows correspond to zero, intermediate, and large t_2, respectively (as in Fig. 3). We see that at zero t_2 the sign of Δ changes, indicating an oscillatory behavior across the tubes. In the LP case when t_2 increases, the oscillating nodes appear in a more off-center region, as discussed for the axial profiles along the tubes. At large t_2, there is no oscillation of Δ across tubes in both LP and HP cases, showing the suppression of FFLO order. We notice in Figs. 3 and 4 that t_2 enhances the maximum magnitude of the gap function, as expected from Eq. (10). This enhancement raises the critical temperature above

which the pairing order vanishes and hence agrees with the increase of the superfluid transition temperature in quasi-1D systems [22].

Finally, we look at the phase separation of fully-paired and fully-polarized regions as a function of t_2. We consider the combined fraction of particles in the highly paired ($s/\rho < 5\%$) and highly polarized ($s/\rho > 95\%$) regions of the axial profiles; $\gamma \equiv \int_z \rho[\theta(0.05 - s/\rho) + \theta(s/\rho - 0.95)]/ \int_z \rho$, where θ is the step function. The larger γ is, the stronger the phase separation the system shows. The panel (a) in Fig. 5 shows that γ monotonically increases with t_2 at three various polarizations when t_1 is fixed. In the cases of $P = 12.5\%$ and 25% the sudden changes indicate the occurrence of the BCS-like center replacing the FFLO center. For comparison we plot also γ vs t_1 at fixed t_2 in panel (b) and observe that γ shows almost no change at the three polarizations. This result highlights that it is t_2, rather than t_1, that accounts for the phase separation and hence is essential for the correct modeling describing the physics at the incipience of the dimensional crossover regime.

V. CONCLUSION

In conclusion, considering the microscopic physics of cold atomic systems, we have incorporated both ST and PT processes to effectively model imbalanced fermionic superfluids in an array of 1D tubes at the incipience of the dimensional crossover. Our calculations show that the PT strength is a main factor for the evolution of the system profiles deviating from the 1D limit, which exhibits a central FFLO state, toward the development of 3D signatures, including a central fully-paired state in the LP case and spatial separation between fully-paired and fully-polarized states in both LP and HP cases. These features are reflected in the directly observed density profiles and the pairing orders which can be probed in time-of-flight experiments [44–47]. Our model can be easily generalized to incorporate higher-order, higher-band or inter-band processes [33, 38], which are expected to be of further help to investigate the system's transition to the continuous 3D limit.

[1] P. Fulde and R. A. Ferrell, Phys. Rev. **135**, A550 (1964).
[2] A. I. Larkin and Yu. N. Ovchinnikov, Zh. Eksp. Teor.

Fiz. **47**, 1136 (1964) [Sov. Phys. JETP **20**, 762 (1965)].
[3] R. Casalbuoni and G. Nardulli, Rev. Mod. Phys. **76**, 263

(2004).

[4] A. I. Buzdin, Rev. Mod. Phys. **77**, 935 (2005).

[5] I. Bloch, J. Dalibard, and W. Zwerger, Rev. Mod. Phys. **80**, 885 (2008).

[6] W. Ketterle and M. W. Zwierlein in *Proceedings of the International School of Physics "Enrico Fermi" in Ultra-cold Fermi Gases, Course CLXIV, Varenna*, edited by M. Inguscio, W. Ketterle, and C. Salomon (IOS Press, Amsterdam, 2008); see also arXiv:0801.2500.

[7] S. Giorgini, L. P. Pitaevskii, and S. Stringari, Rev. Mod. Phys. **80**, 1215 (2008).

[8] L. Radzihovsky and D. E. Sheehy, Rep. Prog. Phys. **73**, 076501 (2010).

[9] M. W. Zwierlein, A. Schirotzek, C. H. Schunck, and W. Ketterle, Science **311**, 492 (2006).

[10] G. B. Partridge, W. Li, R. I. Kamar, Y.-an Liao, and R. G. Hulet, Science **311**, 503 (2006).

[11] Y.-an Liao, A. S. C. Rittner, T. Paprotta, W. Li, G. B. Partrige, R. G. Hulet, S. K. Baur, and E. J. Mueller, Nature (London) **467**, 567 (2010).

[12] T. Mizushima, K. Machida, and M. Ichioka, Phys. Rev. Lett. **94**, 060404 (2005).

[13] D. E. Sheehy and L. Radzihovsky, Phys. Rev. Lett. **96**, 060401 (2006); Ann. of Phys **322**, 1790 (2006).

[14] G. Orso, Phys. Rev. Lett. **98**, 070402 (2007).

[15] X.-Ji Liu, H. Hu, and P. D. Drummond, Phys. Rev. A **76**, 043605 (2007); Phys. Rev. A **78**, 023601 (2008).

[16] A. E. Feiguin and F. Heidrich-Meisner, Phys. Rev. B. **76**, 220508 (2007).

[17] P. Kakashvili and C. J. Bolech, Phys. Rev. A **79**, 041603(R) (2009).

[18] D.-H. Kim, J. J. Kinnunen, J.-P. Martikainen, and P. Törmä, Phys. Rev. Lett. **106**, 095301 (2011).

[19] L. O. Baksmaty, H. Lu, C. J. Bolech, and H. Pu, Phys. Rev. A **83**, 023604 (2011); New J. Phys. **13**, 055014 (2011).

[20] K. Yang, Phys. Rev. B **63**, 140511(R) (2001).

[21] M. M. Parish, S. K. Baur, E. J. Mueller, and D. A. Huse, Phys. Rev. Lett. **99**, 250403 (2007).

[22] E. Zhao and W. V. Liu, Phys. Rev. A **78**, 063605 (2008).

[23] J. P. A. Devreese, S. N. Klimin and J. Tempere, Phys. Rev. A **83**, 013606 (2011).

[24] R. M. Lutchyn, M. Dzero, and V. M. Yakovenko, Phys. Rev. A **84**, 033609 (2011).

[25] K. Sun and C. J. Bolech, Phys. Rev. A **85**, 051607(R) (2012).

[26] A. E. Feiguin and F. Heidrich-Meisner, Phys. Rev. Lett. **102**, 076403 (2009).

[27] D.-H. Kim and P. Törmä, Phys. Rev. B **85**, 180508(R)

(2012).

[28] H. Moritz, T. Stöferle, K. Günter, M. Köhl, and T. Esslinger, Phys. Rev. Lett. **94**, 210401 (2005).

[29] Private communication with R. Hulet.

[30] D. Jaksch and P. Zoller, Annals of Physics **315**, 52 (2005).

[31] C. Chin, R. Grimm, P. Julienne, and E. Tiesinga, Rev. Mod. Phys. **82**, 1225 (2010).

[32] D. B. M. Dickerscheid, U. Al Khawaja, D. van Oosten, and H. T. C. Stoof, Phys. Rev. A **71**, 043604 (2005).

[33] L.-M. Duan, Phys. Rev. Lett. **95**, 243202 (2005); Europhys. Lett. **81**, 20001 (2008).

[34] M. L. Wall and L. D. Carr, Phys. Rev. Lett. **109**, 055302 (2012).

[35] D. Jaksch, C. Bruder, J. I. Cirac, C. W. Gardiner, and P. Zoller, Phys. Rev. Lett. **81**, 3108 (1998).

[36] H. P. Büchler, G. Blatter, and W. Zwerger, Phys. Rev. Lett. **90**, 130401 (2003).

[37] G. M. Bruun and C. J. Pethick, Phys. Rev. Lett. **92**, 140404 (2004).

[38] C. J. M. Mathy and D. A. Huse, Phys. Rev. A **79**, 063412 (2009).

[39] M. Olshanii, Phys. Rev. Lett. **81**, 938 (1998).

[40] P. G. De Gennes, *Superconductivity of Metals and Alloys* (Addison-Wesley, Reading, MA, 1989).

[41] K. Sun, J. S. Meyer, D. E. Sheehy, and S. Vishveshwara, Phys. Rev. A **83**, 033608 (2011).

[42] L. Jiang, L. O. Baksmaty, H. Hu, Y. Chen, and H. Pu, Phys. Rev. A **83**, 061604(R) (2011).

[43] W. Meissner and R. Ochsenfeld, Naturwissenschaften **21**, 787 (1933).

[44] T. Kinoshita, T. Wenger, and D. S. Weiss, Science **305**, 1125 (2004); Nature **440**, 900 (2006).

[45] M. Swanson, Y. L. Loh, and N. Trivedi, New J. Phys. **14**, 033036 (2012).

[46] Hong Lu, L. O. Baksmaty, C. J. Bolech, and Han Pu, Phys. Rev. Lett. **108**, 225302 (2012).

[47] C. J. Bolech, F. Heidrich-Meisner, S. Langer, I. P. McCulloch, G. Orso, and M. Rigol, Phys. Rev. Lett. **109**, 110602 (2012).

[48] Combining with any bare inter-atomic interaction present, one would obtain an effective inter-atomic interaction as discussed in Ref. [32].

[49] The global polarization, P, is defined as the ratio of total imbalance to the total number of particles. The LP case we focus herein is somewhat higher than the critical polarization of 15–18% verified in experiments.